# Predicting the Flexure Response of Wood-Plastic Composites from Uni-Axial and Shear Data Using a Finite-Element Model

Scott E. Hamel, Ph.D., P.E., M.ASCE[1]; John C. Hermanson, Ph.D.[2]; and Steven M. Cramer, Ph.D., P.E., M.ASCE[3]

**Abstract:** Wood-plastic composites (WPCs), commonly used in residential decks and railings, exhibit mechanical behavior that is bimodal, anisotropic, and nonlinear viscoelastic. They exhibit different stress-strain responses to tension and compression, both of which are nonlinear. Their mechanical properties vary with respect to extrusion direction, their deformation under sustained load is time-dependent (they experience creep), and the severity of creep is stress-dependent. Because of these complexities, it is beneficial to create a mechanics-based predictive model that will calculate the material's response in situations that are too difficult or expensive to test experimentally. Such a model would also be valuable in designing and optimizing new structural shapes. Analysis and prediction of WPC members begins with the time-dependent characterization of the material's axial and shear behaviors. The data must then be combined with a tool that can simulate mode-dependence, anisotropy, and nonlinear axial stress distributions that vary over the length of a member and evolve with time. Time-dependent finite-element (FE) modeling is the most practical way to satisfy all of these requirements. This paper presents an FE material model that was developed to predict the deflection of flexural members subjected to both quasi-static ramp loading and long-term creep. Predictions were made for six different WPC products, encompassing a variety of polymers and cross-sections. These predictions were compared with experimental testing and the model shows some success, particularly in the quasi-static response. Creep predictions were more accurate for solid polyethene-based materials than polypropylene-based hollow box sections. **DOI: 10.1061/(ASCE)MT.1943-5533.0001018.** © *2014 American Society of Civil Engineers.*

**Author keywords:** Creep; Wood-polymer composite; Power-law; Finite-element; Abaqus; Flexure; User-defined material model.

## Introduction

Extruded wood-plastic composite (WPCs) members are produced by mixing finely ground wood flour and thermoplastic resin at elevated temperatures, and then extruding the mixture through a die to form structural shapes. A solid rectangle, similar to sawn lumber, is the most common shape, but hollow box extrusions have also been used. The strength, stiffness, cost, and workability of WPC products makes them suited for applications in which wood or wood-based products have traditionally been used. They are currently used predominately in outdoor applications with low structural demands, such as residential decking, deck rails, windows, and fencing (Schildmeyer et al. 2009; Smith and Wolcott 2006). Their prevalence in this area is likely attributable to claims that they exhibit less decay and require less maintenance in moisture rich conditions, which offset their added upfront costs. WPC residential products have historically enjoyed steady market increase; from 1995 to 2005, the WPC decking industry realized a volume growth rate of 30% per year (Klyosov 2007). Their growth coincided with environmental and health concerns surrounding chromated copper arsenate (CCA) treated wood products, which were banned completely from residential construction in 2003 (Jambeck et al. 2007). There has been strong interest in utilizing the structural capacity and subsequently improving both the structural performance and durability of WPC products (Clemons 2002; Smith and Wolcott 2006). For this to occur, though, there must be a reliable method for predicting their performance.

The stress-strain response of WPC's is nonlinear, mode-, time-, and temperature-dependent (Dura 2005; Kobbe 2005; Marklund et al. 2006; Rangaraj and Smith 1999). Despite this complex behavior and a lack of established standards, simplified metrics, such as the ultimate strength or initial modulus of elasticity have been used to quantify their mechanical response to load. Because of their relative strength, stiffness, and cost, new structural WPC products will likely be targeted to replace wood in outdoor applications. Examples of such applications include deck substructures, docks, footbridges, and low volume vehicular bridges, all of which invoke bending as their primary mode of loading. For these structures to be economically competitive, however, the cost must be reduced, the mechanical properties of WPCs must be improved, or they must be reinforced in some manner (Jiang et al. 2007). Some initial studies have already been conducted (Dura et al. 2005; Jiang et al. 2007) to evaluate reinforcement with fiber-reinforced polymers (FRP), but these efforts are limited without a mechanics-based predictive tool that can evaluate various cross-sections and reinforcement schemes. One promising technology uses a belt-press to co-extrude reinforcement with WPC panels (Gardner and Han 2010). Large shapes, however, cannot yet be produced with this method.

There have been a few attempts to create an analytical tool for evaluating the flexure behavior of WPCs. Haiar (2000) developed a

[1]Assistant Professor, Univ. of Alaska Anchorage, 3211 Providence Dr., Anchorage, AK 99508 (corresponding author). E-mail: sehamel@uaa.alaska.edu

[2]Research General Engineer, USDA Forest Products Laboratory, Gifford Pinchot Dr., Madison, WI 53726.

[3]Professor and Associate Dean of Academic Affairs, Univ. of Wisconsin-Madison, Madison, WI 53706.

Note. This manuscript was submitted on September 4, 2013; approved on January 3, 2014; published online on January 6, 2014. Discussion period open until November 30, 2014; separate discussions must be submitted for individual papers. This paper is part of the ***Journal of Materials in Civil Engineering***, © ASCE, ISSN 0899-1561/04014098(9)/$25.00.

Fortran-based program that determined the quasi-static moment-curvature relationship of WPC materials. This routine incrementally increases the extreme fiber compressive strain and then varies the slope of the strain distribution (curvature) through the beam depth until equilibrium is reached. The stress at each strain level is calculated using mode-dependent hyperbolic tangent functions. Time-dependent behavior is not considered. Dura (2005) developed a routine that predicts the time-dependent moment-curvature behavior using the commercial software *Matlab*. This model discretizes the cross-section layers and incrementally increases the curvature. Equilibrium at each curvature is reached by varying the neutral axis location. The constitutive response is also defined using a hyperbolic tangent, and the time-dependence is described using a modified Voigt model. Both of these previous models neglected shear deformation and required incremental steps and iterative solutions to describe the material's behavior. Each of these analytical tools was developed to assist with the addition of fiber-reinforcing to WPC members and was based on the testing of one or two WPC formulations.

The objective of this study was to develop a mechanics-based model that predicts the long-term deflection of wood-plastic composite members subjected to bending. Such a model requires the calculation of the time-dependent axial and shear behaviors, including the nonlinear bimodal response to quasi-static loading and the stress-dependent response to sustained loading.

## Predictive Model and Experimental Procedures

The uniaxial and shear behaviors of the materials were determined through a series of tension, compression, and flexure coupon tests described in Hamel et al. (2013a, b). A description of the predictive model and the experiments conducted to verify the model are presented here.

### *Functional Relationships to Describe the Mechanical Behavior*

WPCs, like the polymers that comprise them, exhibit a bimodal nonlinear viscoelastic response to uniaxial testing. This requires functional relationships that relate time, stress, and strain to describe the material's one-dimensional (1D) mechanical behavior. Like all materials, to fully describe the three-dimensional (3D) material continuum in beam bending, these 1D functional relationships must be combined into a third order tensor that expresses the constitutive relation. In the most general sense, this results in 27 separate constitutive parameters, each of which might be time-dependent, bimodal, nonlinear, and stress-dependent. Clearly, this represents far too many parameters to find experimentally; therefore, a number of simplifying assumptions must be made to approximate the behavior of WPCs.

WPC products are usually thin or thin-walled sections with one dimension that is significantly smaller than the others, allowing the use of the plane-stress condition. There is some evidence that the stiffness in the direction perpendicular to the extrusion direction is less than that parallel to extrusion (Haiar 2000). The intended application of this model, however, is not heavily influenced by biaxial behavior, and any difference between axial moduli was neglected. The moduli functions determined from uniaxial testing parallel to extrusion were used for both the extrusion and normal direction. A sensitivity analysis of this assumption revealed that a 50% reduction in modulus perpendicular to the extrusion direction modified the final bending deflection by less than 2%.

Little work has been conducted on WPCs or thermoplastics to determine if there is interaction between axial stress (strain) and shear strain (stress). One investigation by Ewing et al. (1973) suggests that multidimensional loading of polyethylene can be described by accepted plasticity relationships, which means that the normal and shear responses are independent. It was assumed that this is also true of WPC materials. Applying all of these simplifications, the resulting matrix of stress-strain coefficients used in the tensorial constitutive equation can be expressed with four parameters as

$$\mathbf{C}(\boldsymbol{\sigma}_{\mathbf{ij}}) = \begin{bmatrix} C_a(\sigma_{11}) & C_u(\sigma_{11}) & 0 \\ & C_a(\sigma_{22}) & 0 \\ \text{Sym} & & C_s\left(\sigma_{12}\right) \end{bmatrix} \quad (1)$$

where $C_a$ = axial constitutive relation, $C_s$ = shear constitutive relation in the 12 plane, and $C_u$ describes the interaction effects between stress and strain in the two normal directions.

As a result of the difficulty of describing the constitutive relations of nonlinear-viscoelastic materials, mathematical models have historically been used to approximate the phenomenological behavior of the material (Findley et al. 1989). The semiempirical relations that are used to describe the uniaxial material behavior were presented by Hamel et al. (2013b). For this model, the material's behavior is divided into time-independent and time-dependent components, which are defined and applied separately. The nonlinear incremental stress-strain response for each axial mode is governed by the sum of an exponential relation and a linear term. This is used to find the axial modulus, which is determined by taking the inverse of the derivative of the strain with respect to stress. This results in

$$E_{ii}^{\text{ini}}(\sigma) = \frac{d\sigma_{ii}}{d\varepsilon_{ii}} = \left[\frac{A_0}{\sigma_0} \cdot \text{Exp}\left(\frac{\sigma_{ii}}{\sigma_0}\right) + \frac{1}{E_0}\right]^{-1} \quad (2)$$

where $E^{\text{ini}}$ = time-independent uniaxial tangent modulus, $\varepsilon$ denotes strain, $\sigma$ denotes stress, and $A_0$, $\sigma_0$, and $E_0$, are material dependent constants for each mode.

The biaxial interaction coefficient, $C_u$, is generally quantified as a function of the axial modulus and the time-dependent contraction ratio, $\mu$(t), which is analogous to Poisson's ratio, $\nu$, in time-independent materials. The contraction ratio has been shown to be time-dependent in polymers (Benham and McCammond 1971), however, it is generally accepted (Dean and Broughton 2007; Tschoegl et al. 2002) that the relative change of its value is insignificant, and it can be approximated as a constant. Experimental tests by Dura (2005) determined that the contraction ratio for WPCs is approximately 0.33, which was used for this model. The stress-strain coefficient $C_u$ will vary with the axial modulus, which itself is stress-dependent. Because the moduli in the two normal directions depend on their respective applied stresses, they will differ, and one modulus must be selected at each point to be used to calculate $C_u$. The lesser of the two moduli was chosen for this model, which ensures the largest interaction effect.

The shear constitutive relation, $C_s$, is determined from the shear modulus, G. Because the applied shear stresses in bending are relatively low compared with the shear capacity (Haiar 2000), it was assumed that the reduction in shear modulus attributable to applied stress is negligible. Thus, the initial shear modulus is used throughout the modeling. The plane-stress relations are assembled using the mechanics of elasticity, which results in

$$\mathbf{C}(\boldsymbol{\sigma}_{\mathbf{ij}}) = \begin{bmatrix} \frac{E_{xx}}{(1-\mu^2)} & \frac{-\mu \cdot E_{\min}}{(1-\mu^2)} & 0 \\ \frac{-\mu \cdot E_{\min}}{(1-\mu^2)} & \frac{E_{yy}}{(1-\mu^2)} & 0 \\ 0 & 0 & G \end{bmatrix} \quad (3)$$

where $E_{\min}$ = lesser of the two axial moduli, $\mu$ = contraction ratio, and the axial moduli ($E_{xx}$ and $E_{yy}$) are stress-dependent.

The time-dependent component of the axial behavior is quantified using the time-dependent strain increment. This is expressed as the time-derivative of a power law expression for creep behavior. The derivation of this expression, which can be found in Hamel et al. (2013b), utilizes a power law to describe long-term behavior and an exponential term to describe the zone of transition between quasi-static and creep behavior

$$d\varepsilon_{ii}^{cr} = dt \cdot B(\sigma_{ii}) \cdot \left[ n \cdot t^{(n-1)} + \frac{A_2}{t_1} \cdot Exp\left(\frac{-t}{t_1}\right) \right] \quad (4)$$

where

$$B(\sigma_{ii}) = A_1 \cdot \sigma_{ii}^P \quad (5)$$

$d\varepsilon_{ii}^{cr}$ = axial creep strain increment, $A_1$, $A_2$, $P$ and $n$ are mode dependent material constants, $t_1$ = limit of the transition zone, $t$ = time since the stress was applied, and $dt$ = time increment.

It is likely that the material responds in the same manner when stress is applied in the shear direction as in the axial direction, and the time-dependent portion can be described by Eqs. (4) and (5) with material parameters specific to shear. However, for stress levels less than 50% of the ultimate tensile strength, the ratio of the axial modulus to shear modulus, $\beta$, is approximately constant (Hamel et al. 2013a). This indicates that the time-dependent shear creep strain will be proportional to its axial counterpart, making it unnecessary to determine separate shear parameters by experiment once the moduli ratio, $\beta$ has been determined. The incremental shear creep strain can be found by multiplying the shear stress by $\beta$, and then substituting this equivalent stress into Eq. (4) with the axial the material parameters.

## User-Created FE Constitutive Model

The mechanical behavior of the WPC materials was modeled using a user-created material (UMAT) in the finite-element (FE) software package *Abaqus*. The custom designed UMAT was used to determine the stress response of each element owing to imposed time-dependent deformation.

The UMAT routine imports the 16 user-defined material constants from the FE program. These are the seven constants described in Eqs. (2), (4), and (5) for each mode (tension and compression), and the $\beta$ ratio and contraction ratio, $\mu$. These constants can be found from a program of uniaxial and shear testing, such as those described in (Hamel et al. 2013a, b). During each iterative step, the stresses for each principal direction ($\sigma_{xx}$, $\sigma_{yy}$, $\sigma_{xy}$) are taken from the previous step and applied to find the normal moduli, $E_{ii}$ and the creep coefficients, $B(\sigma_{ii})$, using Eqs. (2) and (5). The time-independent shear modulus G, is determined by multiplying the initial axial stiffness modulus by $\beta$. The creep coefficient for the shear direction, $B(\sigma_{xy})$ is calculated by multiplying the shear stress by $\beta$ and substituting the results into Eq. (5) with tension constants.

Once the moduli for each direction were found, a check is performed to ensure that the modulus in one normal direction is not more than 10 times larger than the other. This constraint, which was adopted from limits on elastic materials in *Abaqus*, is dependent on the contraction ratio and ensures that each element remains stable. If this limit is surpassed, the modulus in the stiffer direction is artificially reduced by equating it to 10 times the modulus in the softer direction. The moduli are also limited so that they remain above 1.0% of the initial tension stiffness. Sensitivity analyses show that varying these limits does not significantly change the solutions of the bending problems investigated.

The routine uses Eq. (4) to determine the time-dependent strain rate $d\varepsilon_c$, (also called the creep strain rate) in each direction. The calculated incremental creep strain is subtracted from the total incremental strain to match the functional constitutive relations. Once the proper incremental strain and element stiffness are determined, they are used to update the stress vector. This stress vector is then passed back to *Abaqus* which then tests the system for equilibrium and updates it using the full Newton method. Further details about the *Abaqus* model and the *UMAT* code can be found in Hamel (2011).

## Experimental Flexure Testing

Flexure testing was conducted to verify the accuracy of the predictive FE model. Experiments were conducted on full-size extruded boards using two different loading conditions: (1) an increasing imposed deflection (displacement-controlled quasi-static), and (2) a steady-state applied force (creep). Edgewise four-point bending tests with a span of 2.13 m were conducted on specimens from each formulation for each loading condition.

To ensure broad applicability, six formulations, each from a different manufacturer, were tested. These represented a range of polymers, wood species, and product cross sections. Four of the formulations (C, D, L, and X) were primarily polyethylene, whereas the remaining two were produced with polypropylene (A and Z). Both polypropylene formulations were extruded as closed box members, whereas the others all had solid rectangular cross-sections. Further details about the materials and the products can be found in Hamel et al. (2013b).

### Quasi-Static Testing

Ten coupon specimens of each formulation with a span-to-depth (L/d) ratio of 16 were subjected to bending to failure. The tests were conducted on a servo–mechanical testing machine in flatwise three-point bending with a span of 165 mm according to ASTM D790 (2003). A monotonically increasing mid-span deflection was imposed to correspond to an extreme fiber strain rate of 1% per minute. The cross-head speed was determined using $\dot{\Delta} = (L^2\dot{\varepsilon})/6d$ where $L$ is the span, d is the depth of the member and $\dot{\varepsilon}$ is the target strain rate. Vertical deflections were measured with $a \pm 12$ mm LVDT and the force was measured using a 450 N load cell. Data was acquired using a *LabVIEW* (National Instruments) data acquisition program at a rate of 4 Hz. Experiments were conducted in an environmentally conditioned room at 25°C and 50% R.H.

In addition, two full-size boards of each formulation were tested to failure under quasi-static loading in four-point bending according to ASTM D6109 (2005a). The 2.13 m span resulted in L/d ratios of approximately 16. The steel loading arm had a span of 610 mm and was hinged at the center where it was connected to the load-cell. Steel rollers and curved contact plates with a curve radius of 610 mm were used at all force and reaction points. Steel rollers and bracing were also used at third-points to prevent the board from deflecting laterally. A servo–mechanical testing machine was used to subject the boards to a constantly increasing displacement corresponding to an extreme fiber strain rate of approximately 1% per min. The cross-head speed was determined using $\dot{\Delta} = (28/135) \cdot (L^2\dot{\varepsilon}/d)$.

TransTek LVDTs with a range of ±50 mm was used to measure the midspan vertical deflection of the cross–sectional centroid. Computerized data acquisition was used to record the data at 5 Hz. The large machine required for the experiments was located in an open testing floor, which was subject to air temperature and

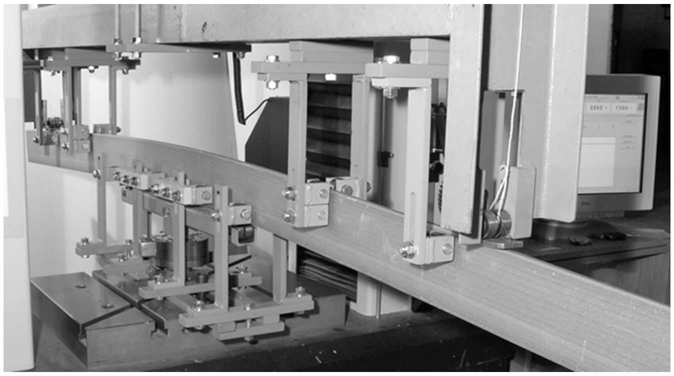

**Fig. 1.** Photograph of quasi-static tests of full-size board (formulation L)

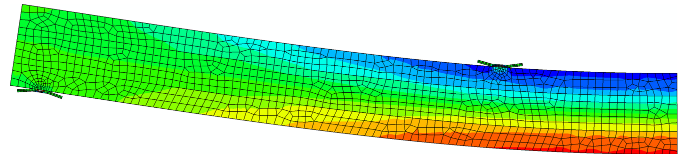

**Fig. 2.** Image of the axial stress intensity for the finite-element model in *Abaqus* for full-size bending simulation of formulation C

humidity fluctuations, though ambient temperatures were approximately equal to 25°C. The humidity conditions during testing are not known, but all specimens were stored in an environmentally controlled chamber at 25°C and 65% R.H. prior to testing. A photo of the test setup can be seen in Fig. 1.

### Creep Testing

Full-size boards were tested under sustained load for three years. The applied forces for the flexure tests were determined such that the flexure-induced axial stresses matched those applied during uniaxial coupon testing. The forces were calculated using a preliminary finite-element model routine similar to the one described in previous sections. Axial tests were performed at 20 and 50% of the average tension failure strength as described in Hamel et al. (2013b). To size the test apparatus, estimations of the three-year creep deflections were calculated as three times the instantaneous deformation. It is recommended for future studies that four-times the deflection be used, as many of the estimates were nonconservative. The loads, deflections, and the corresponding axial tension stresses can be seen in Table 1.

Creep bending tests were conducted according to ASTM D6109 (2005a) and ASTM D6112 (2005b). Two specimens were tested at each of the two stress levels using four-point bending with at 2.13 m span. The specimens, which were the full cross-section of the product and thus varied in size, were conditioned for a minimum of 24 h at the test environment. TransTek LVDTs with ranges between ±12 and ±50 mm were attached to the specimens at midspan to measure the time-dependent vertical deflection. Loads were applied using pneumatic cylinders, which were precisely controlled by electro-pneumatic regulators. Data from the pressure regulators and LVDTs were recorded at intervals that ascended as the creep test progressed. The specimens' loading rate was dependent on the cylinder air pressure, hose size, and length. These varied by formulation and load level, but were generally between 1.5 and 13 kN (350 and 3,000 lbs) per min, with the slower load rates corresponding to tests with low load levels. The experiments were conducted in an environmentally conditioned room at 25°C and 50% R.H.

**Table 1.** Bending Loads and Deflections of Creep Specimens

| Designation | Load level (%) | Tensile stress (MPa) | Full-size flexure load (N) | Quasi-static deflection (mm) |
|---|---|---|---|---|
| A | 20 | 4.48 | 859 | 12.7 |
| | 50 | 11.2 | 2,200 | 33.4 |
| C | 20 | 4.62 | 1,070 | 8.80 |
| | 50 | 11.6 | 2,770 | 25.5 |
| D | 20 | 2.56 | 623 | 4.40 |
| | 50 | 6.41 | 1,590 | 12.2 |
| L | 20 | 2.32 | 249 | 4.40 |
| | 50 | 5.79 | 627 | 11.6 |
| X | 20 | 2.34 | 667 | 10.4 |
| | 50 | 5.86 | 1,780 | 29.7 |
| Z | 20 | 4.14 | 836 | 9.80 |
| | 50 | 10.3 | 2,170 | 27.9 |

### *Finite-Element Modeling Methods*

The *Abaqus* models, which utilized symmetry, were constructed using 2D planar deformable sections meshed with plane-stress elements. Free-form meshing was enabled which created both four-node bilinear quadrilateral (CPS4R) elements and three-node linear triangular (CPS3) elements. Model size varied by formulation, but the full-size beam model generally contained approximately 1,100 elements, of which approximately 5% were triangular. Mesh size was generally approximately 12 mm per side, but decreased around the supports and load points to 2 mm. Support and load was applied through modeled steel supports that were joined to the WPC material across a 20 mm zone. The steel supports were permitted to rotate to simulate the steel rollers in the experimental setup. An image showing the axial stress of the full-size bending model for C-formulation is shown in Fig. 2.

Natural variations in the bending response of the WPC materials were simulated in the FE model by incorporating the range of the materials' axial behavior as input. These variations are present for all wood-plastic composite materials owing to the heterogeneous composition of the material and the mixing and extrusion process. The variation of the axial behavior was quantified using a nonlinear mixed-effect statistical model (Lindstrom and Bates 1990). This analysis assumes that the material behavior exhibits a normally distributed variation that is described by multiple variables. The results of the statistical analyses define the average material constants, their distributions and correlations. As noted, these material constants, which are used in Eqs. (3)–(5), and their coefficients of variation can be found in Hamel et al (2013a, b). The correlations of the variables were similar across all the formulations and are shown in Tables 2 and 3. The fixed-effect parameters (mean response) were used for the time-independent variables in the creep simulations, making the two sets of models (quasi-static and creep) and their associated variables independent.

The statistical program *R* was used to calculate a multivariate normal distribution for each formulation using the distribution and correlation information. These distributions were used to randomly generate a list of 28 sets of material constants, which represent the statistical range of materials' behaviors. Virtual bending tests were

**Table 2.** Correlation of Time-Independent Constants

| Constant | $A_0$ | $\sigma_0$ | $E_0$ |
|---|---|---|---|
| $A_0$ | 1.0 | — | — |
| $\sigma_0$ | 0.95 | 1.0 | — |
| $E_0$ | 0.90 | 0.90 | 1.0 |

**Table 3.** Correlation of Time-Dependent Constants

| Constant | $A_1$ | $P$ | $n$ | $A_2$ |
|---|---|---|---|---|
| $A_1$ | 1.0 | — | — | — |
| $P$ | −1.0 | 1.0 | — | — |
| $n$ | −0.02 | 0.02 | 1.0 | — |
| $A_2$ | 0 | 0 | 0 | 1.0 |

then simulated with the *Abaqus* model using each set of constants, which produced 28 different responses for each of the three test conditions (quasi-static loading and two creep load levels). This was done for each of the six materials for a total of 504 simulations. The resulting range represents the deformation response between the 5th and the 95th percentile with a 75% confidence interval. Evaluating whether the experimental test data were within the distribution of predicted responses provided a measure of the adequacy of the model. This process enabled the repetition of tests that are relatively easy to conduct, such as uniaxial tension, to capture and predict the material variation, while limiting the number of tests that are difficult and expensive, such as full-size bending.

Because of the many assumptions used to create the 3D time-dependent user-programmed material model, it was deemed necessary to verify the model and associated constants. This was done for both the quasi-static and creep conditions by replicating the experimental axial and shear test conditions with the FE model.

## Comparison of Predicted and Measured Results

The large number of formulations and tests conducted in this study prevents the presentation of all the test data and predictions here. Instead, graphical results are presented for formulation C only. The results of all the formulations can be found in Hamel (2011). Formulation C was chosen because, as a coupled HDPE formulation with 55% pine wood flour and a solid cross section, it represents a common commercial product. In addition, the results of formulation C are typical of the results found across the other materials.

### *Quasi-Static Response*

The results of the uniaxial simulation of the quasi-static tests are shown for formulation C in Fig. 3. The test results are well predicted by the FE model, indicating that the material model is effective for axial behavior, and that the dogbone shapes used in the experimental testing result in appropriate material constants. The response predictions deviate from the test data at high stress levels, which is attributable to the upper limit placed on the data range (80% of the average ultimate stress) that was used to determine the modeling constants. This limit was imposed to improve the fit of the mathematical functions on the axial input data at the low stress levels, which were of primary interest.

Quasi-static bending behavior was simulated with the FE model for both three-point bending of coupon specimens and four-point bending of full-sized members. The specimens, loading, and boundary conditions of the experimental setups were simulated as closely as possible in the model. The experimental test data fit within the predicted response range at loads below approximately 50% of the ultimate strength (Fig. 4). This is the range of primary interest because creep rupture will occur in relatively short durations at higher stress levels. The prediction is overly stiff for load levels near failure, which is a direct result of the deviation of the input functions from the axial test data at high stress levels.

Portions of the comparisons shown in Fig. 4(a) can be expressed for all six formulations using a box plot (Fig. 5) of the deflections at specified load levels. This method displays predictions and tested deflections at a particular load level, analogous to cutting a horizontal section through a load-deflection curve like those shown in Fig. 4. The two load levels chosen were 20 and 50% of the average failure load for the experimental coupon bending tests. The midspan deflections for all the experimental and virtual tests were determined at the specified loads, and the deflections were normalized by the mean predicted value. The mean predicted deflection was determined by using the fixed effect parameters only, that is, neglecting the random effects. In some cases, the random generation process produced a slight difference between the median, represented by the line in the *box*, and the mean prediction. The box in the plot represents the range from the 1st to the 3rd quartile, whereas the outside bars represent the minimum and maximum predicted deflections. Experimental values to the left of the mean deflection indicate that the FE model is softer than the tested response.

For most formulations, the test values fall within the range of predicted bending deflections. The experimental values found for

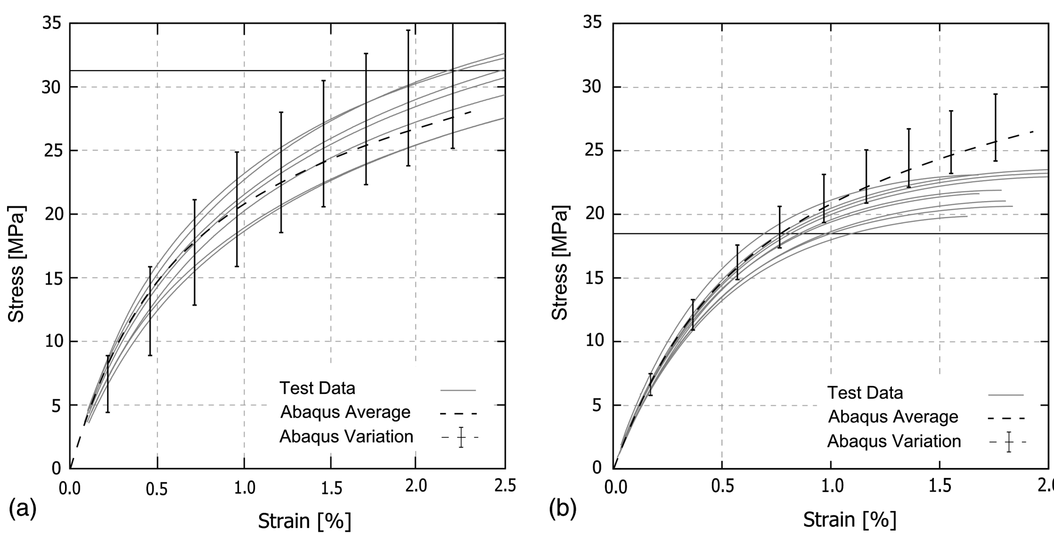


**Fig. 3.** Results of tests and predictions for coupon specimens of formulation C in: (a) compression; (b) tension; horizontal line indicates 80% of the average ultimate strength

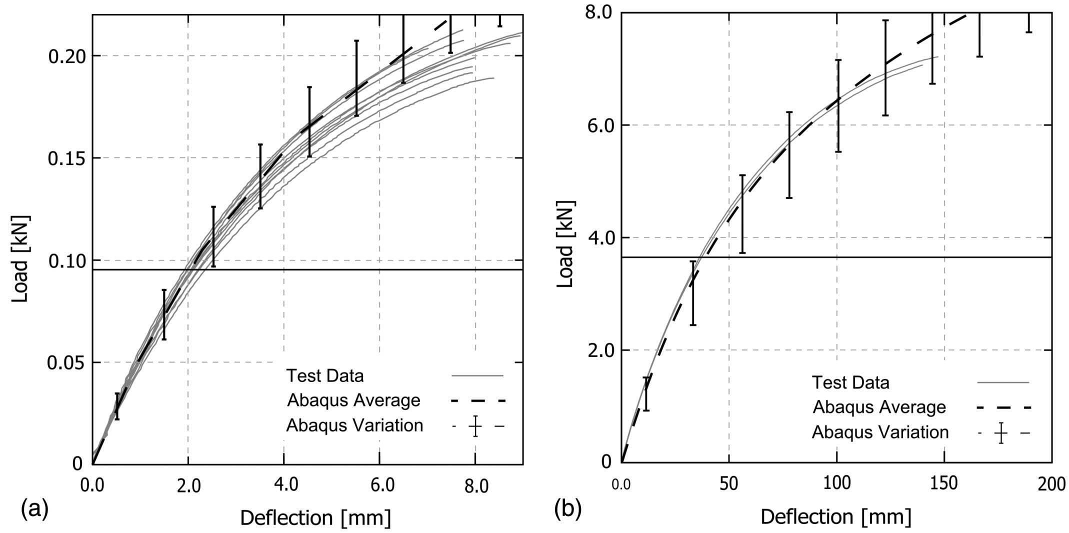


**Fig. 4.** Results of tests and predictions for bending of: (a) coupon specimens; (b) full-size members for formulation C; horizontal lines indicate 50% of the average ultimate strength

formulation A indicate two distinctive behaviors, possibly a result of specimens from different boards or production runs. The softer of these behaviors may have dominated the specimens used to characterize the material, resulting in predictions that are more compatible with the softer boards. The model was also slightly less stiff for formulations Z, though this research formulation had a very narrow material variation in the axial testing. The predicted bending deflections of formulation D were generally larger than the data. The variation in the response of formulation D, however, is relatively large, and the 10 specimens tested in each mode (tension, compression and shear) may have been insufficient to represent this material.

### Long-Term Creep Response

Creep bending behavior was simulated with the FE model for four-point bending of full-sized members. To evaluate the time-dependent model without influence from the quasi-static response to the initial ramp loading, the two responses were separated by subtracting the time-independent response (strain or deflection) from the total deformation. Because of the difficulty in determining the end of the loading period in the pneumatically loaded viscoelastic specimens, the quasi-static response was defined as the deformation 36 s (0.01 h) after the start of the loading.

The time-dependent simulation of the uniaxial coupon specimens revealed a flaw in the compression dogbones used. It was determined that the radius used for the dogbone was too small, and the gage length between tangent points was too short. This geometry had to be chosen early in the testing to minimize buckling before data were available to utilize FE analysis. As a result of the flaw, the stress distribution across the gage length of the specimens was nonuniform, varying by as much as 1,700 kPa and increasing with time. This variation caused the stress levels used to define the $B(\sigma)$ function from the test data to be inaccurate. To remedy this, the necessary material creep constants, $A_1$ and $P$, were determined iteratively using the FE model. The resulting constants used in the bending models, which vary slightly from the tested values published in Hamel et al. (2013b) can be found in Hamel (2011). The results of the axial verification using the revised constants are shown for formulation C in Fig. 6. It should be noted that the compression stresses used in the long-term axial testing, which are not numerically equal to the tension stresses shown in Table 1, were generated from the preliminary FE bending model. Thus, they should match the extreme fiber compression stress in the full-size bending tests. In addition, the tension stresses shown in Fig. 6 vary slightly from the theoretical stress in Table 1 resulting from experimental variation of the applied load. As noted, the load was applied using bladder-style pneumatic cylinders. Although these devices hold a steady load for extended time, they perform poorly at hitting a precise target pressure during initial inflation. In general, the applied stresses are within 1 and 6% of the target values. The loads shown are the measured values, which were also used in the *Abaqus* model. In general, the experimental responses fall within the range of predictions.

The predicted and tested creep deflections over time of full-size members for formulations C are shown in Fig. 7. As with the quasi-static response, portions of the experiment-prediction comparison can be expressed for the six formulations using a box plot (Fig. 8). Three test times were chosen to demonstrate the evolution of the predicted deflection at one load level. The midspan deflections for the experimental and virtual tests at 20% of the ultimate strength

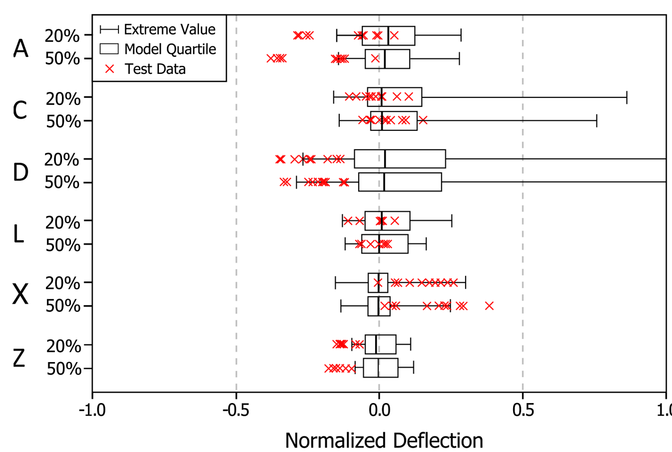


**Fig. 5.** Normalized predicted and experimental deflections at two load levels for coupon bending specimens; +0.5 indicates a tested deflection that is 1.5 times as large as the average prediction, whereas −0.5 indicates a tested deflection that is one half the average prediction

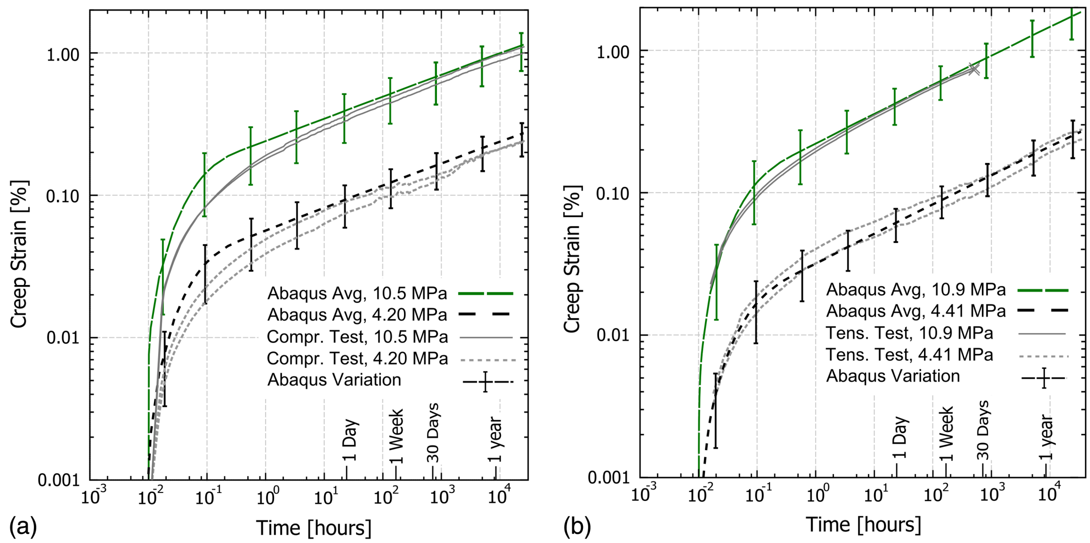


**Fig. 6.** Results of tests and predictions for the creep strain of formulation C in: (a) compression; (b) tension

were determined and normalized by the mean predicted value. It can be seen that for all the products except formulation D, the predicted values are less than the tested deflections. The predictions are most accurate for formulations C, D, and X, which are all polyethylene-based and have rectangular cross sections.

The difference between the tested and the predicted deflections for formulations A, and L are relatively large. Both formulations have unusual cross-section geometries that may have influenced the experimental data. Formulation L has an extremely thin cross-section (12.5 mm) when subjected to edgewise bending, which may have caused out-of-plane warping effects despite efforts to control it. Formulation A has a nonsymmetric box section with an extremely thin compression flange.

### *Simplified Expression for Long-Term Creep*

Eq. (2) was developed to capture the creep behavior of the material at all time scales, but it is sometimes only necessary to predict the creep behavior at long times. In these cases, the time-dependent exponential transition term can be neglected. The result can then be combined with Eq. (4) to describe the strain response to an increasing load followed by a sustained load:

$$\varepsilon(\sigma,t) = \frac{\sigma}{E_0} + A_0\left[\mathrm{Exp}\left(\frac{\sigma}{\sigma_0}\right) - 1\right] + A_1 \cdot \sigma^P \cdot t^n \qquad (6)$$

The relative difference between the sum of Eqs. (2), and (4), and Eq. (6) can be evaluated at various timescales using the predictive FE model. The time-dependent midspan deflections of full-size WPC members subjected to four-point bending was determined using the FE model programmed with each of the two constitutive models. These deflections and the percent difference between them are shown in Table 4.

Results show that the difference between the predicted deflections after three years is less than 5% for all formulations, and many are significantly lower. This difference is lower than one quartile

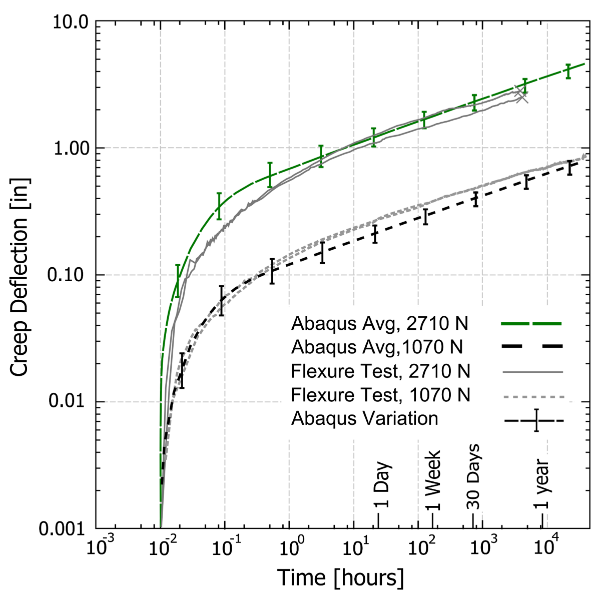


**Fig. 7.** Results of tests and predictions for full size flexure tests of formulation C

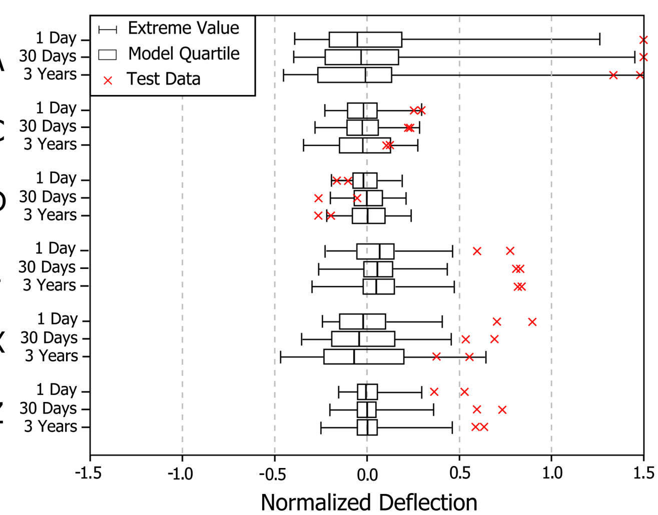


**Fig. 8.** Normalized predicted and experimental creep deflections for bending of full size members at 20% of ultimate strength; +0.5 indicates a tested deflection that is 1.5 times as large as the average prediction, whereas −0.5 indicates a tested deflection that is one half the average prediction

**Table 4.** Predicted Deflection (mm) of Full Size Bending Specimens for Each Formulation at 20% of $\sigma_u$

| | 30 days | | | Three years | | |
|---|---|---|---|---|---|---|
| Designation | With transition | No transition | Percentage error (%) | With transition | No transition | Percentage error (%) |
| A | 17.9 | 17.6 | 1.3 | 26.7 | 26.5 | 0.9 |
| C | 19.8 | 18.6 | 6.2 | 29.2 | 28.0 | 4.1 |
| D | 13.6 | 13.2 | 2.8 | 22.2 | 21.8 | 1.8 |
| L | 8.2 | 8.0 | 2.3 | 12.6 | 12.4 | 1.4 |
| X | 18.1 | 17.1 | 5.8 | 27.4 | 26.3 | 4.0 |
| Z | 20.6 | 20.1 | 2.2 | 32.5 | 32.1 | 1.3 |

of the simulated variation of each material, as shown in Fig. 8. Such an insignificant variation indicates that for situations in which only the long-term creep deflection is necessary, Eq. (6) can be used successfully.

## Discussion

The predictive model is based on known principles of mechanics and mathematical representations of tension, compression, and shear data. The experimental data fall within the range of responses predicted by the model, which uses a statistical distribution of the material constants, for the following situations:

- Quasi-static ramp loading of tension and compression dogbones below 80% of the ultimate strength (Fig. 3)
- Quasi-static ramp loading of small beam coupons subjected to bending [Fig. 4(a)]
- Creep loading of tension and compression dogbone specimens (Fig. 6)

Situations were modeled accurately for some, but not all, of the WPC formulations, these include:

- Quasi-static ramp loading of full size flexure members [Fig. 4(b)]
- Creep loading of the full-sized flexure members (Fig. 7)

The predicted response of the quasi-static ramp loaded full-size members subjected to bending was generally less stiff than the test data, that is, the model over-predicted deflections for a specified load. This was especially noticeable at higher loads. The predicted creep response of full-sized members subjected to bending was stiffer than the test data, which indicates that the model under-predicted the creep deflections. The discrepancy was less consistent across the formulations than that of the quasi-static response, and was most pronounced in formulation A, the asymmetric polypropylene box section. The discrepancy of the creep response far outweighed that of the quasi-static response and dominated the total deflection behavior in time-dependent tests. A comparison of the predicted and experimental total deflections is shown in Fig. 9. Predictions using a simple *rule of thumb* estimation method used in timber design (two times the initial quasi-static deflection), and a modification of this rule are also shown. In some cases, the experimental results fall outside the range of deflections predicted by the FE model (formulations D and Z). The model and associated variation, however, provide a more accurate prediction of the tested behavior for five of the six formulations than the simple estimate of three times the initial deflection after three years of creep.

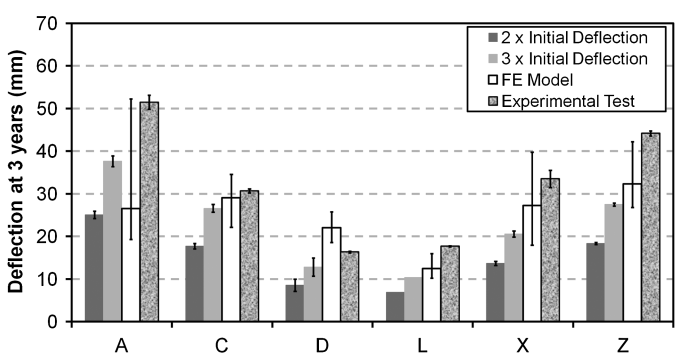


**Fig. 9.** Predicted and experimental creep deflections for bending of full size members at 20% of ultimate strength; error bars indicate the maximum and minimum values from 28 simulated tests or two experimental tests

One potential cause for the observed discrepancies is variation of the mechanical properties over the cross-section of the extruded member. In this study, the experimental data were collected for extreme fiber zones only, and it was assumed, based on previous research (Adcock et al. 2001), that variation over the cross-section was negligible. However, more recent research (Dura 2005) has concluded that depending on the production method and the material, the properties may vary significantly over the cross-section. Preliminary work indicates that this is also true of some of the products in this study, particularly formulation D. In addition, there are other phenomena that may stiffen the full cross-section during ramp loading, such as the presence of a surface skin or internal residual stresses, which are not accounted for in the current mechanics-based model.

The stress dependency of the creep response, in combination with the stress variation over the cross-section during bending, causes the shape of stress distribution to evolve over time as the various strain rates and equilibrium conditions interact. One of the purposes of using a time-dependent FE model is to capture this phenomenon, which it does. However, the model reveals that the creep process results in a *flattening* of the stress distribution: the stress decreases at the extreme fibers, while increasing in the core. Because no experimental work was conducted on either the strain response of a stress decrease (recovery), or the stress decrease attributable to a constant strain (relaxation), it is unlikely that the user-created routine is modeling this behavior correctly, thus introducing errors.

It was also found during modeling that deep beams (low L/d ratio) are sensitive to both boundary conditions, and the theoretical assumptions about biaxial relationships, thus reducing the accuracy of models of these situations.

Improvements to the model can be realized with further development in:

- Characterization of the strain recovery attributable to a stress decrease, and stress relaxation owing to a sustained strain.
- Rate-dependent quasi-static response.
- Time-dependent anisotropic interactions.
- Effects of residual stresses and cross-section variation that occur in full size sections.

The challenge of describing this material's behavior is evident by the difficulty of even this relatively intricate model to accurately describe its bending response in all situations. It is clear that WPCs exhibit extremely complex behavior and cannot be described by simple linear-elastic theories.

## Conclusions

A predictive model was developed to describe the mechanical response of wood-plastic composites. This model takes the form of a user-programmed FE model based on the principles of mechanics and the results of uniaxial and shear testing. Considiering the dearth of prior experimental data and modeling efforts of WPC materials, this research was aimed at testing and modeling a relatively wide range of behaviors and formulations. It was not intended to determine and describe all of intricacies of an anisotropic nonlinear viscoelastic material.

The model showed some success in describing the response of beams in bending for quasi-static ramp loading and long-term creep. In five of the six formulations, the model provided a better prediction of the deflections than simple estimation methods. The average percent error between the model and experimental results across all formulations for the total bending deflection after three years of sustained load was 25%, compared with 50% using a simple estimate of two times the initial deflection.

## Acknowledgments

This research was supported by the National Research Initiative of the USDA Cooperative State Research, Education and Extension Service (grant number 2005-35103-15230).

## Supplemental Data

Tables S1–S3 are available online in the ASCE Library (www.ascelibrary.org). These tables present the material constants that were used to generate the predicted behaviors shown in Figs. 3–8.

## References

*Abaqus version 6.9* [Computer software]. Velizy-Villacoublay, France, Dassault Systemes.

Adcock, T., Hermanson, J. C., and Wolcott, M. P. (2001). "Relationship between extrusion parameters and wood-plastic composite properties, engineered wood composites for naval waterfront facilities." *Project End Rep.*, Washington State Univ., Pullman, WA.

ASTM. (2003). "Standard test methods for flexural properties of unreinforced and reinforced plastics." *D790*, West Conshohocken, PA, 11.

ASTM. (2005a). "Standard test method for flexural properties of unreinforced and reinforced plastic lumber and related products." *D6109*, West Conshohocken, PA.

ASTM. (2005b). "Standard test methods for compressive and flexural creep and creep-rupture of plastic lumber shapes." *D6112*, West Conshohocken, PA, 7.

Benham, P. P., and McCammond, D. (1971). "Studies of creep and contraction ratio in thermoplastics." *Plast. Polym.*, 39(140), 130–136.

Clemons, C. (2002). "Wood-plastic composites in the United States: The interfacing of two industries." *For. Prod. J.*, 52(6), 10–18.

Dean, G. D., and Broughton, W. (2007). "A model for nonlinear creep in polypropylene." *Polym. Test.*, 26(8), 1068–1081.

Dura, M. (2005). "Behavior of hybrid wood-plastic composite—fiber reinforced polymer structural members for use in sustained loading applications." M.S. thesis, Univ. of Maine, Orono, ME.

Dura, M., Lopez-Anido, R. A., Dagher, H., Gardner, D., O'Neill, S., and Stephens, K. (2005). "Experimental behavior of hybrid wood-plastic composite fiber-reinforced polymer structural members for use in sustained loading applications." *8th Int. Conf. on Wood and Biofiber Plastic Composites*, Forest Products Society, Madison, WI, 131–137.

Ewing, P. D., Turner, S., and Williams, J. G. (1973). "Combined tension-torsion creep of polyethylene with abrupt changes of stress." *J. Strain Anal. Eng. Des.*, 8(2), 83–89.

Findley, W. N., Lai, J. S., and Onaran, K. (1989). *Creep and relaxation of nonlinear viscoelastic materials: With an introduction to linear viscoelasticity*, Dover, Dover, NY.

Gardner, D. J., and Han, Y. (2010). "Towards structural wood-plastic composites: Technical innovations." *Proc., 6th Meeting of Nordic-Baltic Network in Wood Material Science and Engineering (WSE)*, Tallinn Univ. of Technology Press, Tallinn, Estonia, 7–21.

Haiar, K. J. (2000). "Performance and design of prototype wood-plastic composite sections." M.S. thesis, Washington State Univ., Pullman, WA.

Hamel, S. E. (2011). "Modeling the time-dependent flexural response of wood-plastic composite materials." Ph.D. dissertation, Univ. of Wisconsin–Madison, Madison, WI.

Hamel, S. E., Hermanson, J. C., and Cramer, S. M. (2013a). "Mechanical and time-dependent behavior of wood-plastic composites subjected to bending." *J. Thermoplast. Compos. Mater.*, in press.

Hamel, S. E., Hermanson, J. C., and Cramer, S. M. (2013b). "Mechanical and time-dependent behavior of wood-plastic composites subjected to tension and compression." *J. Thermoplast. Compos. Mater.*, 26(7), 968–987.

Jambeck, J., Weitz, K., Solo-Gabriele, H., Townsend, T., and Thorneloe, S. (2007). "CCA-treated wood disposed in landfills and life-cycle tradeoffs with waste-to-energy and MSW landfill disposal." *Waste Manage.*, 27(8), S21–S28.

Jiang, L., Wolcott, M., Zhang, J., and Englund, K. (2007). "Flexural properties of surface reinforced wood/plastic deck board." *Polym. Eng. Sci.*, 47(3), 281–288.

Klyosov, A. A. K. (2007). *Wood-plastic composites*, Wiley-Interscience, Hoboken, NJ.

Kobbe, R. G. (2005). "Creep behavior of a wood-polypropylene composite." M.S. thesis, Washington State Univ., Pullman, WA.

*LabVIEW 8.2* [Computer software]. Austin, TX, National Instruments.

Lindstrom, M., and Bates, D. (1990). "Nonlinear mixed effects models for repeated measures data." *Biometrics*, 46(3), 673–687.

Marklund, E., Varna, J., and Wallstrom, L. (2006). "Nonlinear viscoelasticity and viscoplasticity of flax/polypropylene composites." *J. Eng. Mater. Technol.*, 128(4), 527–536.

*Matlab* [Computer software]. Natick, MA, Mathworks.

Rangaraj, S. V., and Smith, L. V. (1999). "The nonlinearly viscoelastic response of a wood-thermoplastic composite." *Mech. Time-Depend. Mater.*, 3(2), 125–139.

Schildmeyer, A. J., Wolcott, M. P., and Bender, D. A. (2009). "Investigation of the temperature-dependent mechanical behavior of a polypropylene-pine composite." *J. Mater. Civ. Eng.*, 10.1061/(ASCE)0899-1561(2009)21:9(460), 460–466.

Smith, P., and Wolcott, M. (2006). "Opportunities for wood/natural fibre-plastic composites in residential and industrial applications." *For. Prod. J.*, 56(3), 4–11.

Tschoegl, N. W., Knauss, W. G., and Emri, I. (2002). "Poisson's ratio in linear viscoelasticity–A critical review." *Mech. Time-Depend. Mater.*, 6(1), 3–51.